

Magnetic properties of Quantum Corrals from 'first principles' calculations

B. Lazarovits^{††}, B. Újfalussy[‡], L. Szunyogh^{†§}, B. L. Györfy^{†*} and P. Weinberger[†]

Abstract. We present calculations for electronic and magnetic properties of surface states confined by a circular quantum corral built of magnetic adatoms (Fe) on a Cu(111) surface. We show the oscillations of charge and magnetization densities and the possibility of the appearance of spin-polarized states. In order to classify the peaks in the calculated density of states with orbital quantum numbers we analyzed the problem in terms of a simple quantum mechanical circular well model. This model is also used to estimate the behavior of the magnetization and energy with respect to the radius of the circular corral. The calculations are performed fully relativistically using the embedding technique within the Korringa-Kohn-Rostoker method.

[†]Center for Computational Materials Science, Technical University Vienna, A-1060, Gumpendorferstr. 1.a., Vienna, Austria

[‡]Metals and Ceramics Division, Oak Ridge National Laboratory, Oak Ridge, Tennessee 37831, USA

[§] Department of Theoretical Physics and Center for Applied Mathematics and Computational Physics, Budapest University of Technology and Economics, Budafoki út 8, H-1111, Budapest, Hungary

* H. H. Wills Physics Laboratory, University of Bristol, Bristol BS8 1TL, United Kingdom

1. Introduction

Over the past two decades, electrons in two dimensional surface states on closed packed surfaces of noble metals have been at the center of much experimental and theoretical attention [1, 2]. For a pristine surface the energies of such states lay in the 'gap' around the L-point of the bulk Brillouin Zone and the wavefunctions are confined to the surface. The corresponding dispersion relations have been determined by angle resolved photoemission spectroscopy and they have been found to be two dimensional free-electron-like parabolas [1, 3]. Moreover, they are partially filled and hence the electrons, which fill them, form a two dimensional metal. The most interesting feature of this remarkable state of matter is its response to perturbations such as caused by placing transition metal atoms on the surface. As might be expected such response displays long range, 'Friedel like', charge oscillations governed by the 2d Fermi 'Surface'. Indeed, one of the iconic experiments in nanotechnology have been the fabrication of a circular arrangement of 48 Fe atoms on a Cu (111) surface and the direct observation, by Scanning Tunneling Microscopy (STM), of such oscillations within the circle [4, 5, 6]. In his paper we wish to discuss the, as yet unexplored, magnetic properties of such Quantum Corrals.

[†] To whom correspondence should be addressed. E-mail: bl@cms.tuwien.ac.at

Until recently STM studies of atoms on well defined Cu, Ag and Au (111) surfaces imaged only the charge distribution of the surface electrons [4, 5, 6]. But now, remarkable developments in spin polarized STM [7] make the observing of spatial variations in the magnetic density a distinct possibility and therefore an attractive new area of research. Evidently, this opens up the possibility of building magnetic nano-structures for both scientific and technological purposes. For instance, while the observation of a single Fe or Co atom on a Cu surface may be beyond the spatial resolution of the first generation of SPSTMs the magnetic state of a single QC of 50-100 atoms can be readily identified [8]. The motivation behind the theoretical work reported here is the need to identify the principle conceptual issues which govern the physics, in general, and the magnetism, in particular, of such structures.

Individual impurities and clusters of impurities embedded in the above surface-2d-host-metals have been studied for Friedel oscillations around them [9, 10], for RKKY interactions between them [11, 12, 13] and for a rich variety of Kondo resonances they are host to [6, 14, 15, 16]. Clearly all these effects can occur inside a corral with the interesting aspect that now the electronic structure of the host can be controlled by the geometry of the corral. It is perhaps useful to note that these circumstances are rather analogous to that of quantum wells in semiconductor physics.

In the semiclassical limit the states of the Quantum Corrals, can be associated with classical orbits of particles bouncing off confining walls. Depending on the shape of the corral the classical motions may be integrable or chaotic. Thus, Quantum Corrals can serve as examples of Quantum Chaos at work [17, 18].

Clearly, to think about using different impurities, different substrates and/or different confining geometries one needs simple but reliable models as guides. In the unfamiliar physical circumstances at hand an efficient way to such models is to perform large scale 'first-principles' calculations including all conceivably relevant effects and in interpreting the results in terms of simple models. This is the approach we take in the present paper. Our 'first-principles' calculations are spin-polarized and relativistic generalizations of the pioneering work of Hormandinger and Pendry [2] and Crampin and collaborators [19, 20] and we interpret the results in terms of a flat bottom 'circular potential well' model. To illustrate the power of this approach, once it has been established that the model faithfully reproduces the main features of the results from 'first-principles' calculations, properties which would be too difficult to calculate from first principles were estimated.

2. Method of calculations

Within multiple scattering theory of the electronic structure the information about each atom (scattering center) is coded in the scattering path operator (SPO) matrix, $\boldsymbol{\tau}(E) = \{\boldsymbol{\tau}^{nm}(E)\} = \{\boldsymbol{\tau}_{QQ'}^{nm}(E)\}$, with Q and Q' being angular momentum indices referring to atomic sites whose position vectors are labeled by n and m respectively and E being the energy. For scatterers described by non-overlapping muffin-tin potential wells

$$\boldsymbol{\tau}(E) = [\boldsymbol{t}^{-1}(E) - \boldsymbol{G}(E)]^{-1} \quad , \quad (1)$$

th SPO describes the full hierarchy of scattering effects between any two particular sites, n and m . In Eq. (1), $\boldsymbol{t}(E) = \{\boldsymbol{t}^n(E) \delta_{nm}\} = \{t_{QQ'}^n(E) \delta_{nm}\}$ and $\boldsymbol{G}(E) = \{\boldsymbol{G}^{nm}(E)\} = \{G_{QQ'}^{nm}(E)\}$ denotes the single-site t -matrices on the energy shell and

the real-space structure constants, respectively. For more details, especially, how to calculate $t_{QQ'}^n(E)$ within a fully relativistic spin-polarized scheme, see, e.g., Ref. [22].

We begin our investigations by two fully self-consistent calculations one for a semi-infinite Cu with a (111) surface and another one for a single Fe ad-atom on a semi-infinite host. In both cases there are Cu sites and two layers of sites which are either the Fe site or sites without a nuclear charge. We call the latter ones empty sites but we note that they do contain electric charge and their electrostatic potential is calculated fully self-consistently. We then construct 'crystal potentials' for further single pass, one-electron calculations following the recipe: all Fe sites are described by the potential, within the atomic sphere surrounding the Fe impurity, in the single impurity calculation, and all other sites are described by the appropriate potentials in the pristine surface calculation. The configurations of interest are those in which empty sites forming the walls of a corral, in the first layer above the last Cu layer, are replaced by Fe sites as shown in Fig. 1. Clearly, by this construction, at the level of the 'crystal potential', we are neglecting the influence of neighboring Fe atoms on each other. This frozen potential approximation was shown to be reasonable in the case of Fe adatoms on Ag(100) [23].

For a given 'crystal potential' constructed according to the above recipe we solve the multiple scattering problem by the embedding method [23]. In short we embed a cluster of sites labeled \mathcal{C} , consisting of the corral Fe atoms and the enclosed space empty sites, in the unperturbed semi-infinite Cu host. A particular cluster \mathcal{C} can then be treated as perturbation of the host. In practice, we first calculate the SPO of the 2D translational invariant layered host, $\tau_h(\mathbf{k}_{\parallel}, E) = \{\mathcal{I}_h^{pq}(\mathbf{k}_{\parallel}, E)\}$ within the framework of the SKKR method[24], where p and q denote layers and the \mathbf{k}_{\parallel} are vectors in the surface Brillouin zone (SBZ). The real-space SPO is then given by

$$\mathcal{I}_h^{mn}(E) = \frac{1}{\Omega_{SBZ}} \int_{SBZ} e^{-i(\mathbf{T}_i - \mathbf{T}_j)\mathbf{k}_{\parallel}} \mathcal{I}_h^{pq}(\mathbf{k}_{\parallel}, E) d^2k_{\parallel} \quad , \quad (2)$$

where the atomic position vectors are decomposed as $\mathbf{R}_m = \mathbf{T}_i + \mathbf{c}_p$ and $\mathbf{R}_n = \mathbf{T}_j + \mathbf{c}_q$ with \mathbf{T}_i and \mathbf{T}_j being 2D lattice vectors, \mathbf{c}_p and \mathbf{c}_q the so-called layer-generating vectors, and Ω_{SBZ} is the unit area of the surface Brillouin zone.

By replacing the t -matrices of the unperturbed host, $t_h(E)$, with those of the cluster-atoms, $t_{\mathcal{C}}(E)$, leads to the following Dyson like equation,

$$\tau_{\mathcal{C}}(E) = \tau_h(E) [\mathbf{I} - (t_h^{-1}(E) - t_{\mathcal{C}}^{-1}(E))\tau_h(E)]^{-1} \quad , \quad (3)$$

where $\tau_{\mathcal{C}}(E)$ is the SPO-matrix corresponding to all sites in cluster \mathcal{C} , from which in turn all corresponding local quantities, i.e., charge and magnetization densities, spin- and orbital moments, as well as the total energy can be calculated. Note, that Eq. (3) takes into account all scattering events both inside and outside the cluster.

2.1. Geometries of interest

The 48 Fe atoms forming the corral were positioned on the surface along a circle with a diameter of $28a$ where a is the two dimensional lattice constant of the fcc(111) Cu surface. The investigated geometry is shown in the inset of Fig. 1. This is similar to a popular experimental one [4]. The corral sites refer to the positions of an ideal fcc parent lattice with the experimental Cu lattice constant, therefore there is some deviation from the exact circular shape. The positions of the adatoms were chosen such that the spacing between them approximately accounts to a constant.

Within the interior of the corral the physical properties (DOS, MDOS) of 55 empty spheres along a diameter were calculated. Note that the rotational symmetry of the considered structure is not continuous. Nevertheless, to reduce the computational effort we followed Crampin *et al.* [19] and assumed that the properties on an arbitrary position within the corral depend only on the distance from the center of the circle.

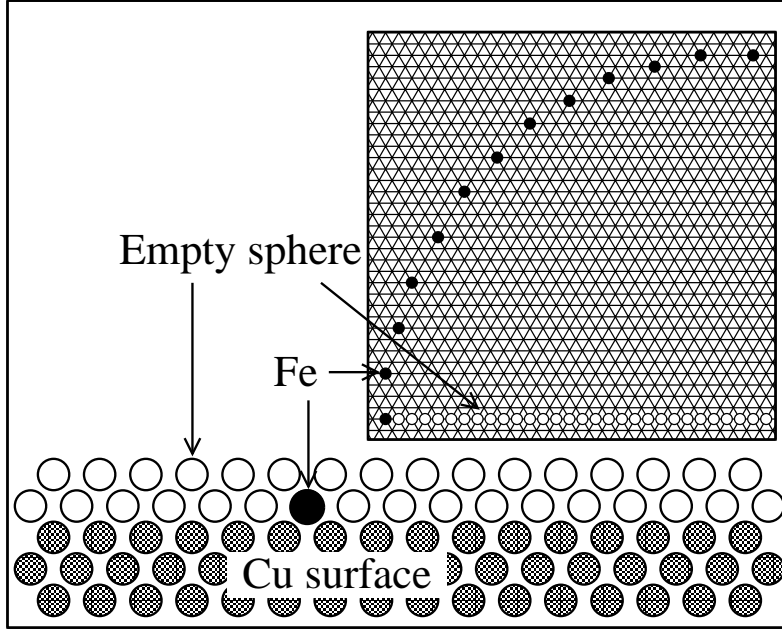


Figure 1. Cross section of the surface showing the position of the "vacuum layers" (open circles), the Cu surface layers (full gray circles) and an Fe impurity within the first "vacuum layer" (full black circles). Inset: the positions of the Fe atoms (black dots) and the empty spheres along a diameter (open circles) for a quadrant of the investigated corral.

2.2. Computational details

Self-consistent, fully relativistic calculations for the Fe adatom on Cu(111) have been performed in the framework of the local spin-density approximation as parameterized by Vosko *et al.* [26] with a magnetization pointing along the z axis (normal to the planes of atoms) as well as for the calculations of the surface-state properties. The potentials were treated within the atomic sphere approximation (ASA). For the calculation of the t -matrices and for the multipole expansion of the charge densities, necessary to evaluate the Madelung potentials, a cut-off of $\ell_{max} = 2$ was used. In order to perform the energy integrations, 16 points on a semicircular contour in the complex energy plane were sampled according to an asymmetric Gaussian quadrature. Both, for the self-consistent calculation of the Cu(111) surface and for the evaluation of Eq. (2) we used 70 k_{\parallel} -points in the irreducible wedge of the SBZ. The DOS and MDOS were calculated at an energy mesh parallel to the real axis with an imaginary part of 0.5 mRyd. In order to cover the surface-states properties properly about 3300 k_{\parallel} points within the IBZ were used for the BZ integration.

3. Results of first-Principles Calculations

3.1. Clean Cu(111) surface

In order to determine the dispersion relation and the effective mass of the surface electrons the Bloch-spectral function (BSF) [22] was calculated between the $\bar{\Gamma}$ and \bar{K} in the fcc(111) BZ close to the Fermi energy by using the SKKR method in which the properties of semi-infinite substrate is calculated by the surface Green function method [24]. The proper treatment of the host is necessary in order to take into account the interaction between the bulk and surface states in an ab-initio way. The maxima of the BSF can be identified as the surface state band. In agreement with the experiments the calculated dispersion relation is free-electron like and can be estimated with a parabola as indicated by Fig. 2. The bottom of the calculated surface states, ϵ_B , band is 0.3 eV below the Fermi energy which is a bit smaller than the experimental values (0.4 eV) [1, 3]. By using a parabolic approximation for the dispersion relation

$$\epsilon_{\mathbf{k}} = \epsilon_B + \frac{\hbar^2 k^2}{2m^*} + \dots \quad (4)$$

we obtained that the effective mass with $m^*/m_e = 0.37$ which is in good agreement with the experimental value [1].

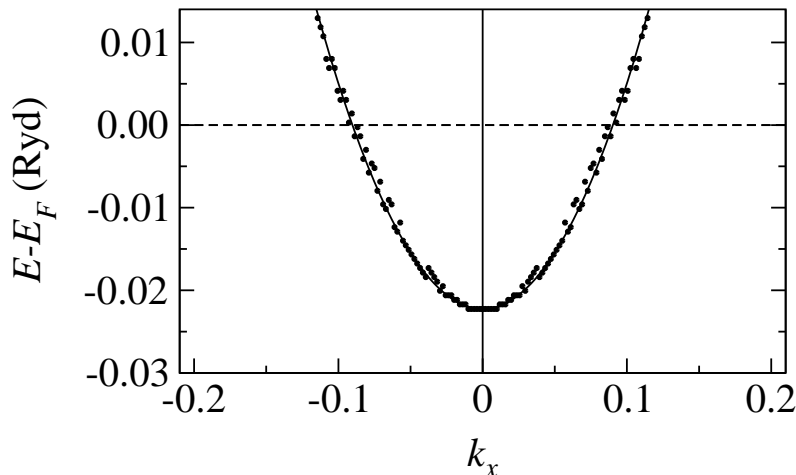


Figure 2. Dots: Bloch spectral function maxima near to the $\bar{\Gamma}$ point of the SBZ. Line: parabola fitted to the calculated maxima. It should be noted that only the first third of the SBZ is displayed ($\bar{K} \approx 0.65$). The estimated effective mass is $m^*/m_e = 0.366$.

3.2. Fe impurity on a Cu(111) surface

In these calculations the magnetic moment on the Fe impurity on the surface turned out to be $3.27 \mu_B$ and its preferred orientation was perpendicular to the surface. The energy of this anisotropy was 4.3 meV. Both of these results are consistent with those already reported in the literature [25]. In all further calculations the Fe adatoms were assumed to be spin-polarized in the z-directions perpendicular to the surface.

3.3. DOS of confined surface states

In order to study the properties of surface states confined by the quantum corral first we investigated the local density of states (LDOS)

$$n_i(E) = n_{i,\uparrow}(E) + n_{i,\downarrow}(E) = -\frac{1}{\pi} \sum_{\sigma=\uparrow,\downarrow} \text{ImTr}G_{\sigma\sigma}^{ii}(E) \quad (5)$$

and the local magnetic density of states (LMDOS)

$$m_i(E) = n_{i,\uparrow}(E) - n_{i,\downarrow}(E) \quad (6)$$

of an "empty sphere" at various lattice points (sites) labeled by i within the corral where $G_{\sigma\sigma}^{ii}(E)$ is the site and spin diagonal part of the resolvent in (l, m, σ) representation. Although in our relativistic theory the spin is not a good quantum number, and hence $G_{\sigma\sigma}^{ii}(E)$ is not diagonal in the empty spheres, we can interpret the diagonal elements in a similar manner as in a non-relativistic theory because within an "empty sphere" the spin-orbit coupling is bound to be small. In Fig. 3. we show the LDOS and LMDOS at the center of the corral.

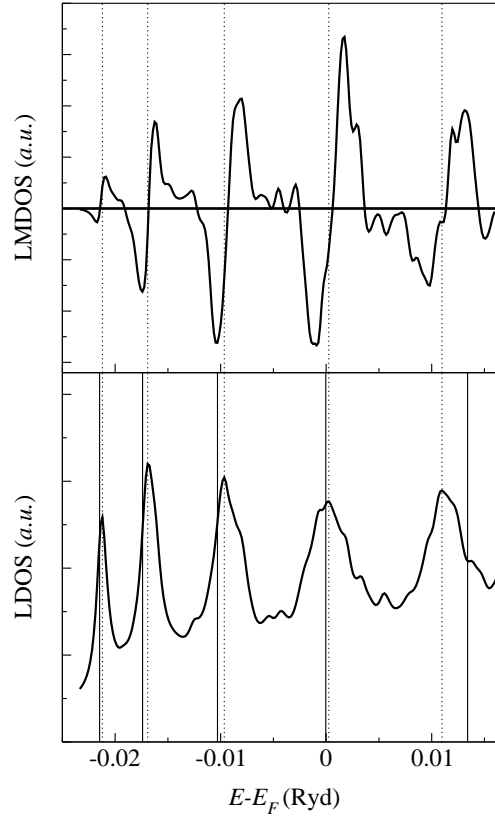


Figure 3. Calculated density of states (LDOS) and magnetic density of states (LMDOS) at the center of a quantum corral. The dotted lines indicate the maxima in the LDOS. Vertical full lines are the energy eigenvalues E_{0i} predicted by the box model.

The striking by peaky structure in Fig. 3. is in sharp contrast to the constant 2d density of states expected from the dispersion relation in Eq. (4). However, the

peaks are rather similar to the results of Crampin et al [19] who interpreted the peaks as 'bound states' within the corral. Somewhat surprising is that the coherent scattering from the circular arrangement of Fe impurities is equivalent to that of an almost infinite confining potential wall. Evidently, such confined states are analogous to the quantum well states in semiconductor physics. In contrast to Crampin *et al.* [19] we have also calculated the spin resolved densities of states LMDOS which are also presented in Fig. 3. Clearly, the LMDOS is more structured than the LDOS suggesting that the quantum well states are exchange split. To lend further evidence to such an interpretation we calculated the spatial distribution of the density of states. The sum of such densities of states along the diameter of the corral is presented in Fig. 4. The results at selected energies corresponding to the most prominent peaks are shown in Fig. 5. and for the fifth peak the LDOS for the whole area within the corral is depicted in Fig. 6. Note that the oscillations continue outside the corral. This implies that the states we have really been studying are not so bound states but rather resonances. The obtained pattern for the confined surface electrons agrees well with the experimental one. Although the local density of state measures the square of the wavefunction at a given energy, and is not the same as the local wave function. The oscillations with distance from the center in Fig. 5. strongly support the interpretation that the selected peak positions are those of bound state confined by the corral.

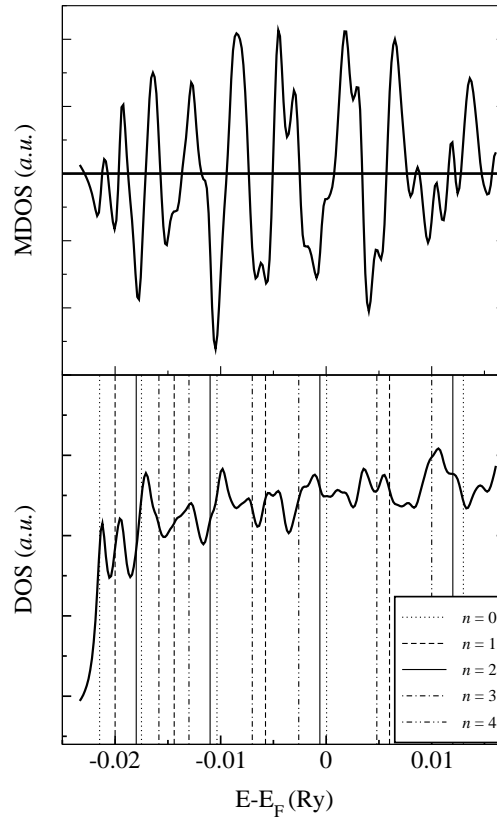


Figure 4. Calculated density of states (DOS) and magnetic density of states (MDOS) summarized for a diameter of the corral. Vertical lines are the energy eigenvalues predicted by the box model corresponding to the value n .

Evidently, even for the present very simple geometry the results are too complicated to allow an identification of each structure with specific physical processes. To maximize the information gained from our 'first-principles' calculations we shall now introduces a simple model whose parameters can be so chosen such that it reproduces most of the above results quantitatively.

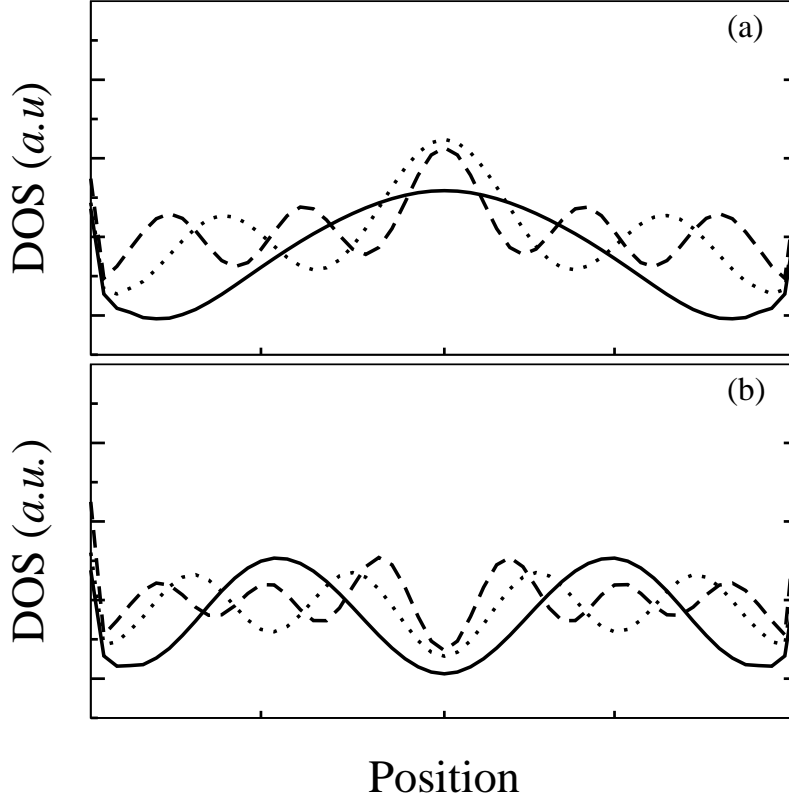


Figure 5. Spatial distribution of the DOS at energies corresponding to the first three peaks of the states which can be identified as $n = 0$ (Figure a) and as $n \neq 0$ (Figure b). The full, dotted and dashed line refer to the first, second and third peak, respectively.

3.4. The Circular Quantum Well model

The circular quantum well model is defined by a potential of the form

$$V(\mathbf{r}) = \begin{cases} 0 & \text{if } r < R \\ +\infty & \text{if } r \geq R \end{cases} \quad (7)$$

It should be recalled that the radial solutions of the corresponding Schrödinger equation are Bessel function of the first kind $J_n(pr)$ where

$$p = \sqrt{\frac{2m^*}{\hbar^2} E} \quad . \quad (8)$$

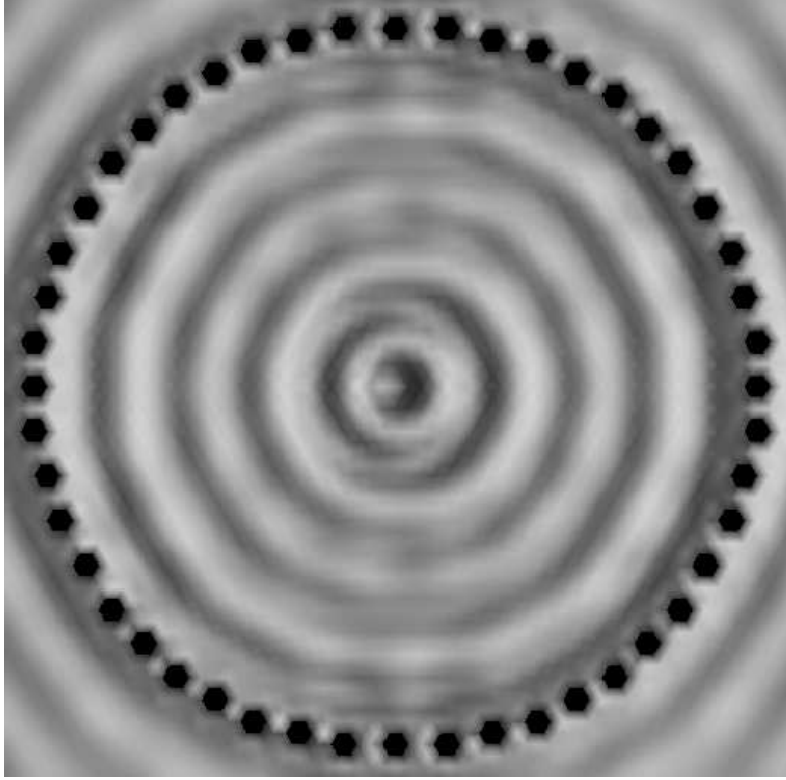


Figure 6. Spatial distribution of DOS at energies corresponding to the fifth peak of the LDOS at the central position. The LDOS on the Fe atoms are removed from the figure.

The energy eigenvalues arise from the boundary condition that the radial solutions vanish at the boundary:

$$E_{ni} = \frac{x_{ni}^2}{R^2} \frac{\hbar^2}{2m^*} \quad , \quad (9)$$

where x_{ni} refer to the i th zero of the Bessel function J_n . In order to investigate the magnetic properties of this model one can generalize it by adding a spin dependent part so that $V_{\uparrow(\downarrow)}(r) = V(r) + U_{i,\uparrow(\downarrow)}$ where the constant $U_{i,\uparrow} = -U_{i,\downarrow}$ can also depend on the quantum number n . The magnetic exchange term modifies the energy values as follows

$$E_{ni}^{\uparrow(\downarrow)} = \frac{x_{ni}^2}{R^2} \frac{\hbar^2}{2m^*} + U_{i,\uparrow(\downarrow)} \quad . \quad (10)$$

In order to facilitate a comparison with the ab-initio results the $R = 27 a$ is used. This means that the radial solution has to vanish at the lattice position neighboring the corral atoms. The corresponding energy values with and without magnetic exchange term for $n = 0$ can be seen in Fig. 7a.

3.5. Interpretation of the results of first-principles calculations

In what follows we comment on the results of our 'first-principles' calculations in the light of the above 'circular well' model. Firstly, we note that in Fig. 3. we

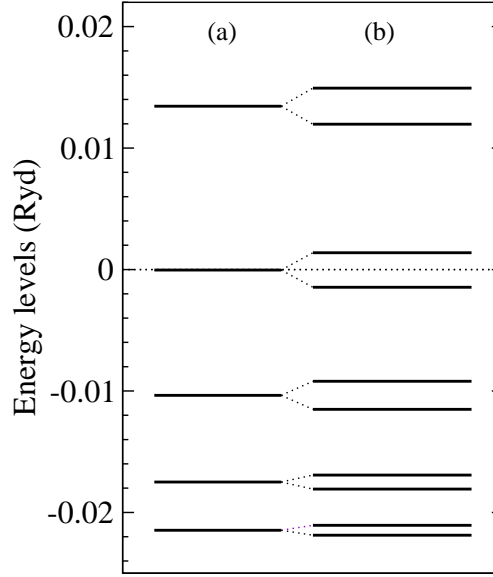


Figure 7. (a): Energy levels of the $n = 0$ states within the box model at the radius used for the self-consistent calculation. (b): Energy levels of the $n = 0$ states within the box model extended by a spin-splitting term at the same geometry. The energy dependent splitting between the spin-up and spin-down states is estimated from the MDOS calculations.

have indicated the bound state energies E_{0i} for $m^*/m_e = 0.37$ and $U_{i,\uparrow(\downarrow)} = 0$. The striking agreement between the peak positions and the E_{0i} 's is especially strong in the low-energy regime. This can be viewed take as an indication that at lower energies the scatterers act more like a hard wall than at higher energies. In the 'first-principles' calculations the peaks have finite widths due to the combined effects of the discreteness of the confining boundary and the energy dependent scattering into bulk states. Remarkably, the width of the peaks agrees quantitatively with the experimental values [27]. For reasons that is not entirely clear, in the experiments the 3rd peak is the highest one but in our result the 2nd.

The spatial distribution of $n_i(E)$ is plotted in the upper panel of Fig. 5. at energies referring to by the first three peaks along a diameter of the corral. As can be expected the LDOS has a maximum at the center similarly to the $J_{n=0}$ Bessel function. The circular well model suggests that there are states with non-zero orbital moment, $n \neq 0$, for which there is a minimum at the center of the corral. In order to find these states we investigated the spatial sum of the LDOS along a diameter

$$n(E) = \sum_i n_i(E), \quad m(E) = \sum_i m_i(E) \quad . \quad (11)$$

These sums are shown in Fig. 4. Near to Fe atoms the LDOS can change more significantly due to the direct charge transfer, therefore in the sum the contributions from the empty spheres neighboring Fe atoms are neglected. Reassuringly, in Fig. 4. there are new peaks as compared with Fig. 3. The values E_{ni} are also presented up to $n = 4$. Note, for example, that the second peak clearly corresponds to the E_{11} state of the 'circular well' model. To pursue this matter further, in the lower panel of Fig. 5, we plotted the spatial density of the states corresponding to those peaks which appear

only in the summed DOS and have a minimum at the center. For higher energies this correspondence is not so clear, nevertheless, this comparison serves as an explanation why the shape of the peaks differs from that of an ideal Lorentzian. The small features between the prominent peaks which can be seen in Fig. 3, and in the experimental results [4] also show some systematic trends which we assume can be explained with a the 'circular well' model based on a 2-dimensional Dirac equation.

Turning to the LMDOS at the central position, we note that in the upper panel in Fig. 3 the prominent DOS peaks are split into a pair of 'up' and 'down' peaks. This oscillatory behavior of the LMDOS is a consequence of the spin-polarization of the corral Fe atoms, namely of the perturbation of the surface-state electrons by the Fe atoms forming the corral with respect to the spin orientation. This exchange splitting can be reproduced in the 'circular well' model by choosing $U_{i,\uparrow(\downarrow)}$ appropriately. It turns out that for a good fit $U_{i,\uparrow(\downarrow)}$ should be non-uniform in energy. The corresponding energy values with the exchange splitting terms estimated from Fig. 3. are shown in Fig. 7b. Thus, the prediction of the model is that if the Fermi energy falls between an exchange split doublet then the whole corral has a net magnetic moment of one Bohr magneton in addition to the magnetization due to the Fe atoms forming the wall. Furthermore, such a moment will not be uniformly distributed within the corral but varies from empty-cell to empty-cell as required by the wavefunction of the confined surface state: it oscillates like the charge density in Fig. 5. Of course, even for a relatively small corral of $R = 27 a$, as indicated by the highly structured summed LMDOS in the upper panel of Fig. 4, there are many states near the Fermi energy and hence the local magnetic moment can vary rapidly with Fermi energy and spacial location. Some of the complexities in this figure can be attributed to the appearance of the $n \neq 0$ states. Although the exchange splitting around the DOS peaks can be clearly observed a full analysis of its structure will have to be based on a treatment using a relativistic model.

3.6. Tuning of the magnetic properties

From the point of view of engineering corrals with specific properties it is important to investigate the magnetic properties of the confined surface states within the corral as functions of the corral radius R . As a preliminary effort in this direction we shall now make some estimates based on the model whose credibility we have established in the previous sections. Firstly, we have calculated the dependence of the exchange split energy levels, shown in Fig. 7 for the specific case of $R = 130.41 a.u.$, as functions of R . The results are displayed in Fig. 8. Assuming that the exchange energies are independent from the geometry we used the values estimated from Fig. 3. It can be seen that as the radius is decreased the energy levels are pushed upwards, possibly changing the number of the occupied states. As a consequence of this effects one can find ranges of radii where the spin-down state is occupied but the corresponding spin-up one is empty and therefore the surface states hold a finite magnetic moment. The predicted total magnetic moment of the surface states is depicted in the inset of Fig. 8. It should be stressed that the model neglects a multitude of effects such as the partial confinement of the electrons and the width of the levels. In realistic 'first principles' calculations the magnetic moment is expected to show a smoother change with the radius. When states with $n > 0$ are also taken into account the results are expected to be much more complicated but the basic effect does not change. At the center of the corral one can expect from Fig. 4 that it is enough to take into account

the $n = 0$ states. Therefore, we can predict that at least at the center there is a finite magnetic moment at well defined geometries. In short, by varying the geometry a rich variety of magnetic states can be produced.

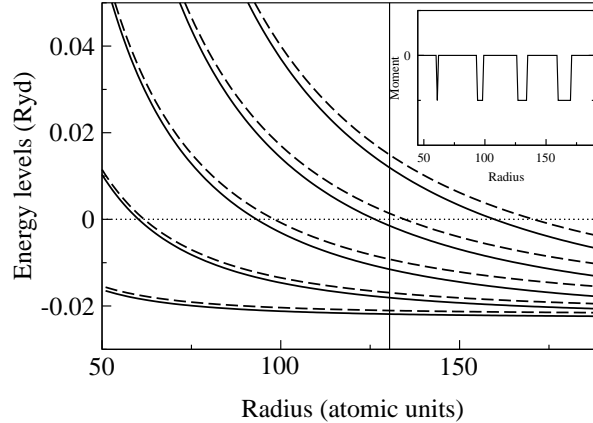


Figure 8. The $l = 0$ energy levels with spin splitting (dashed line: spin-up states, full lines: spin-down states). Inset: Value of the magnetization with respect to the radius within the box model due to the $n = 0$ states. The energy dependent splitting between the spin-up and spin-down states is estimated from the MDOS calculations. The vertical line indicates the radius used for the ab-initio calculation.

As might be expected by now the total energy also shows an interesting behavior by varying the corral radius. As a simple, and perhaps artificial, example we have studied the case when symmetry constrains the system such that only the $n=0$ states are occupied. The total energy for this case is shown in Fig. 9. The oscillations resemble and have similar origin as those responsible for the deHaas-vanAlpen effect. Note, however, that in the present example the oscillations are not equally spaced but follow from the distribution of the Bessel zeros.

4. Summary

In this work we presented calculations of the electronic and magnetic properties of the surface states confined in a circular quantum corral. The ab-initio results are interpreted in terms of a simple quantum mechanical, circular potential well model with infinitely high walls. We found that at low energies the energy levels of the model gave a good quantitative account of the peaks in DOS of ab-initio calculations. In particular, unlike previous calculations for the Quantum Corrals, we were able to study and interpret the magnetic as well as the charge oscillations within the corral. On the basis of these calculations we conclude that a rich variety of magnetic structures can be expected by varying the shape and size of these fascinating nano-structures.

Acknowledgments

Financial support was provided by the Center for Computational Materials Science (Contract No. GZ 45.531), the Austrian Science Foundation (Contract No. W004), the Research and Technological Cooperation Project between Austria and Hungary

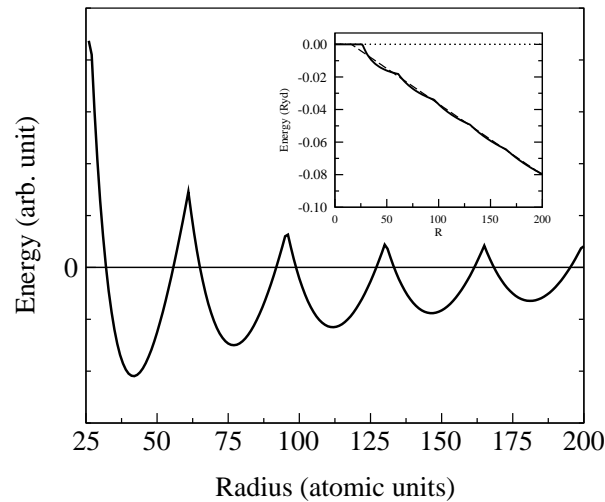


Figure 9. Oscillation in the total energy with respect to the radius within the box model due to the $n = 0$ states. Within the inset the total energy and its best linear fit ($R > 25a.u.$) are plotted by full and dashed line, respectively. In the main figure the difference between the total energy and its linear fit are depicted in order to a better representation of the oscillations.

(Contract No. A-3/03) and the Hungarian National Scientific Research Foundation (OTKA T046267 and OTKA T037856). The work of BU was supported by DOE-OS, BES-DMSE under contract number DE-AC05-00OR22725 with UT-Battelle LLC.

References

- [1] S.D. Kevan, *Phys. Rev. Lett.* **50**, 526 (1983)
- [2] G. Hörmandinger and J. B. Pendry, *Phys. Rev. B* **50**, 18607 (1994)
- [3] F. Baumberger, T. Greber, and J. Osterwalder *Phys. Rev. B* **64**, 195411 (2001)
- [4] M. F. Crommie, C. P. Lutz, D. M. Eigler and E. J. Heller, *Physica D* **83**, 98 (1995)
- [5] M. F. Crommie, C. P. Lutz, D. M. Eigler and E. J. Heller, *Surface Science* **361/362**, 864 (1996)
- [6] H. C. Manohoran, C. P. Lutz, and D. M. Eigler, *Nature* **403**, 512 (2000)
- [7] M. Bode, *Rep. Prog. Phys.* **65**, 523 (2003)
- [8] O. Pietzsch, A. Kubetzka, M. Bode, and R. Wiesendanger *Phys. Rev. Lett.* **92**, 057202 (2004)
- [9] L. Petersen, P. T. Sprunger, Ph. Hofmann, E. Lgsgaard, B. G. Briner, M. Doering, H.-P. Rust, A. M. Bradshaw, F. Besenbacher, and E. W. Plummer, *Phys. Rev. B* **57**, R6858 (1998)
- [10] L. Diekhöner, M. A. Schneider, A. N. Baranov, V. S. Stepanyuk, P. Bruno, and K. Kern, *Phys. Rev. Lett.* **90**, 236801 (2003)
- [11] Jascha Repp, Francesca Moresco, Gerhard Meyer, and Karl-Heinz Rieder *Phys. Rev. Lett.* **85**, 2981 (2000)
- [12] N. Knorr, H. Brune, M. Epple, A. Hirstein, M. A. Schneider, and K. Kern, *Phys. Rev. B* **65**, 115420 (2002)
- [13] V. S. Stepanyuk, A. N. Baranov, D. V. Tsvilin, W. Hergert, P. Bruno, N. Knorr, M. A. Schneider, and K. Kern, *Phys. Rev. B* **68**, 205410 (2003)
- [14] D. Porras, J. Fernández-Rossier, and C. Tejedor, *Phys. Rev. B* **63**, 155406 (2001)
- [15] Gregory A. Fiete, Jesse S. Hersch, Eric J. Heller, H. C. Manohoran, C. P. Lutz, and D. M. Eigler, *Phys. Rev. Lett.* **86**, 2392 (2001)
- [16] Oded Agam, and Avraham Schiller, *Phys. Rev. Lett.* **86**, 484 (2001)
- [17] Gregory A. Fiete, and Eric J. Heller, *Phys. Rev. Lett.* **75**, 933 (2003)
- [18] Eyal Doron, and Uzy Smilansky, *Nonlinearity* **5**, 1055 (1992)
- [19] S. Crampin, O. R. Bryant, *Phys. Rev. B* **54**, R17367 (1996)
- [20] S. Crampin, M. H. Boon and J. E. Inglesfield, *Phys. Rev. Lett.* **73**, 1015 (1994), Henry K.

- Harburya, and Wolfgang Porod, *Phys. Rev. B* **53**, 15455 (1996), S. Crampin, *J. Electron. Spectrosc. Relat. Phenom.* **109**, 51 (2000), J. Kliewer, R. Berndt, and S. Crampin, *Phys. Rev. Lett.* **85**, 4936 (2000), *New J. Phys.* **3**, 22.1 (2001),
- [21] M. F. Crommie, C. P. Lutz, and D. M. Eigler, *Nature* **363**, 524 (1993)
- [22] P. Weinberger, *Electron Scattering Theory for Ordered and Disordered Matter* (Clarendon, Oxford,1990).
- [23] B. Lazarovits, L. Szunyogh, and P. Weinberger, *Phys. Rev. B* **65**, 104441 (2002)
- [24] L. Szunyogh , B. Újfalussy, and P. Weinberger, *Phys. Rev. B* **51**, 9552 (1995)
- [25] B. Lazarovits, L. Szunyogh, P. Weinberger, and B. Újfalussy, *Phys. Rev. B* **68**, 024433 (2003)
- [26] S. H. Vosko, L. Wilk, and M. Nusair, *Can. J. Phys.* **58**, 1200 (1980)
- [27] M. F. Crommie, C. P. Lutz, and D. M. Eigler, *Science* **262**, 262 (1993)